Fifth International Conference on CFD in the Process Industries
CSIRO, Melbourne, Australia
13-15 December 2006

ELECTROMAGNETIC CONTROL OF A TRANSITIONAL BOUNDARY LAYER

Thomas ALBRECHT[1], Roger GRUNDMANN[1], Gerd MUTSCHKE[2], and Gunter GERBETH[2]

[1]Institute for Aerospace Engineering, Technische Universität Dresden, D-01062 Dresden, Germany
[2]Institute of Safety Research, Forschungszentrum Rossendorf, P.O. Box 51 01 19, D-01314 Dresden, Germany

ABSTRACT

We investigate numerically the transition to turbulence in a flat-plate boundary layer controlled by electromagnetic forces. The fluid considered is incompressible, Newtonian and low electrically conductive. Similar to boundary layer suction, when applying a steady, wall-parallel, and streamwise oriented Lorentz force, the Blasius velocity profile is transformed to an exponential one. Since the critical Reynolds number increases to by two orders of magnitude, Transition to turbulence is delayed, and finally drag is reduced.
Direct numerical simulation (DNS) of both linear (2D) and nonlinear (3D) stages of the transition process were performed, as well as a linear stability analysis (LSA) of the intermediate velocity profiles. The obtained results confirm the expected increased stability of the controlled flow. Transition to turbulence is delayed by either damping primary instability, or, in the nonlinear case, by suppressing the emerge of Omega-vortices which usually preceeds the breakdown to turbulence. Surprisingly, our calculations suggest interesting stability characteristics of the intermediate velocity profiles. The decay rate of small disturbances in DNS is maximum in a region near the onset of control and decreases as the velocity profile evolves towards the exponential shape. In LSA, critical Reynolds numbers of intermediate profiles are found to be larger than for the exponential profile.

NOMENCLATURE

a	actuator's stripe size	x,y,z	spatial coordinates
$\mathbf{B}$	magnetic field	Z	Lorentz f. amplitude
c	complex eigenvalue		
$\mathbf{E}$	electric field	α	wave number
$\mathbf{e}_x$	unit vector	δ	displacement thickn.
F^+	frequency parameter	κ	mapping parameter
f	frequency	μ	magn. permeability
$\mathbf{f}_L$	Lorentz force density	ν	kinematic viscosity
H_{12}	shape parameter	ρ	fluid density
$\mathbf{j}$	electr. current density	σ	growth rate
j_0	applied $\mathbf{j}$	σ_E	electr. conductivity
M_0	magnetization		
p	pressure	Subscript indices:	
t	time		
Re	Reynolds number	c	critical
Re_M	magnetic Reynolds	exp	exponential profile
$\mathbf{u}$	velocity = (u,v,w)	in	inflow
U_∞	reference velocity	rms	root mean square

INTRODUCTION

Much effort has been devoted to laminar flow control (see, e.g. the review by Joslin, 1998). A very common actuation is homogeneous suction, where the flat plate boundary layer asymptotically evolves into a velocity profile of exponential shape. Since the critical Reynolds number increases from 519 to $O(50000)$ while suppressing further boundary layer growth, transition to turbulence is substantially delayed, thus reducing drag. Recent experimental work by Fransson and Alfredsson (2003) has reported a large stabilizing effect of suction on both Tollmien-Schlichting (TS) type of instability and on transition induced by free-stream turbulence. If the fluid under consideration is weakly electrically conducting, such as sea water in naval applications, a properly designed Lorentz force can achieve similar results as proposed by Gailitis and Lielausis (1961). Electromagnetic actuation in general has recently received a renewed consideration, mainly aimed at drag reduction in a turbulent boundary layer (Pang and Choi, 2004, Lee and Kim, 2002, Du et al., 2002).
The stability of intermediate profiles developing during transition from Blasius to the asymptotic suction profile was studied first by Ulrich (1944) who found a monotonically increasing critical Reynolds number. Tsinober and Shtern (1967) have investigated the shape of the intermediate velocity profiles due to electromagnetic actuation, but, to our knowledge, the stability properties of these profiles have not yet been studied.
In this paper, we address the question of how a streamwise Lorentz force affects the stability of a transitional boundary layer. Since the early, linear stages of transition are strictly 2D, we study the control influence on emerging TS waves by 2D direct numerical simulation (DNS), where the flow field is assumed to be uniform in spanwise direction. A linear stability analysis (LSA) of intermediate velocity profiles is performed. Late-stage, non-linear transitional structures are investigated by means of 3D calculations.

MODEL DESCRIPTION

Governing Equations

We consider the flat plate boundary layer flow of an incompressible, Newtonian fluid of low electrical conductivity. The Navier-Stokes equation, nondimensionalized using free-stream velocity U_∞ and inflow displace-

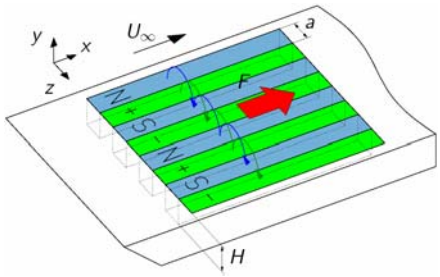

Figure 1: Actuator Design.

ment thickness δ_{in} as characteristic scales, then read

$$\frac{\partial \mathbf{u}}{\partial t} + (\mathbf{u}\,\nabla)\mathbf{u} = -\nabla p + \frac{1}{\mathrm{Re}_{in}}\nabla^2\mathbf{u} + \mathbf{f}_L, \qquad (1)$$

where $\mathrm{Re}_{in}= U_\infty\,\delta_{in}/\nu$ is the inflow Reynolds number and ν represents the kinematic viscosity. Within conductive media, a Lorentz force

$$\mathbf{f}_L = \mathbf{j} \times \mathbf{B} \qquad (2)$$

arises from nonparallel electric and magnetic fields, where **j** is the electric current density and **B** is the magnetic field. The current density is determined by Ohm's law in moving media

$$\mathbf{j} = \sigma(\mathbf{E} + \mathbf{u} \times \mathbf{B}). \qquad (3)$$

Given a weak electrical conductivity $\sigma_E=O(5$ S/m), the induced current $\sigma_E(\mathbf{u}\times\mathbf{B})$ is small. In order to achieve a reasonably high Lorentz force, an external electric field **E** must be applied which dominates eq. (3). Consequently, eq. (2) simplifies to $\mathbf{f_L}=\sigma_E\mathbf{E}\times\mathbf{B}$. Furthermore, assuming a permeability of vacuum $\mu=4\pi10^{-7}$ Hm, the magnetic Reynolds number $\mathrm{Re_M}=\mu\sigma_E\nu\mathrm{Re}$ is in the order of 10^{-9}. Thus, the low induction approximation holds, where **B** can be calculated as if the fluid was at rest (Moreau, 1990). Now, both **E** and **B** are determined by the shape of the actuator only. As shown in Fig. 1, we use an array consisting of streamwise aligned, alternating stripes of permanent magnets and electrodes of changing magnetization orientation and polarity, respectively, flush mounted with the flat plate's surface. Assuming a large stripe aspect ratio, Avilov (1998) calculated electric and magnetic fields analytically, yielding a wall-parallel, purely streamwise oriented Lorentz force. Averaged in spanwise direction, the nondimensionalized force density finally reads

$$\mathbf{f}_L = (\mathrm{Z}\pi^2)/(a^2\mathrm{Re}_{in})exp(-\pi y/a)\,\mathbf{e}_x. \qquad (4)$$

It is exponentially decaying in wall-normal direction with the maximum found at the wall and a controlling the penetration depth of the force. We would like to mention that Avilov, Weier, Mutschke, and Gerbeth (1999) found this force distribution also directly, i.e. without spanwise averaging, by slightly modifiying the actuator design. The dimensionless control amplitude $Z=(j_0M_0a^2)/(8\pi\rho U_\infty\nu)$ describes the ratio of Lorentz and viscous forces, with j_0, M_0, and ρ denoting the applied current density, the magnetization of the permanent magnets, and the fluid density, respectively. If Z equals unity, momentum loss resulting from friction is just balanced by momentum input due to Lorentz forcing, and any initial velocity

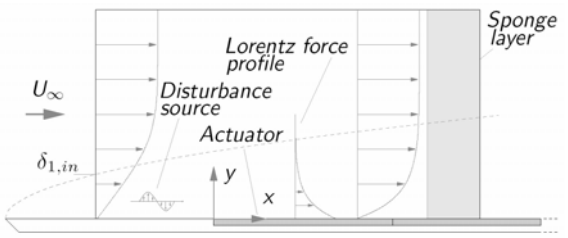

Figure 2: Computational Domain

profile will evolve towards the exponential one. Its asymptotic displacement thickness $\delta_{exp}=a/\pi$ is again determined by the stripe width a. For the studies presented here, a=3.34 is chosen, ensuring shortest transition length from Blasius to the exponential profile, which occurs if the local displacement thickness δ of the Blasius profile right at the beginning of the actuator is approximately 1.4 times the displacement thickness of the asymptotic exponential profile δ_{exp} (Kneisel, 2004).

Direct Numerical Simulation

The governing equations are integrated using a well-established spectral element solver originally developed by Henderson and Karniadakis (1995) which has already been applied to various MHD problems, e.g. Posdziech and Grundmann (2001), Mutschke et al. (2006). Schematically shown in Fig. 2, the rectangular computational domain extending over 990 units in streamwise direction x and 65 units in wall-normal direction y was decomposed into 594 elements of polynomial degree 9. A no-slip condition $\mathbf{u}$=0 at the bottom wall and outflow conditions $(\mathbf{u}\cdot\nabla)\mathbf{u}$ = 0 at both downstream and free-stream boundary were applied. Additionally, to prevent any unphysical reflections at the outflow boundary, the sponge region technique of Guo, Adams, and Kleiser (1996) is used. At inflow x=-200, a Blasius profile of Re_{in}=360 is chosen, and electromagnetic control starts at the origin x=0. For uncontrolled flow, the local displacement thickness δ increases up to 3.0, yielding a local Reynolds number of Re=1080 at the outflow boundary. Similar to Fasel (2002), small amplitude disturbances $0.5<F^+<4$ of nondimensional frequency $F^+=(2\pi f\nu/U_\infty^2)*10^4$ are introduced near the inflow boundary by means of an oscillating body force, creating TS waves of initial amplitude $u_{rms}\approx0.0006$ which propagate downstream.

The local amplitude of a TS wave is then determined by finding the maximum root mean square value $\hat{u}_{\mathrm{rms}}$ of the streamwise velocity component over the wall-normal direction at given downstream position x. To distinguish between stable and unstable flow, a spatial growth rate $\sigma=d/dx\ \ln(\hat{u}_{rms})*100$ is computed, where σ=0 indicates neutral stability.

Linear Stability Analysis

In order to get further insight into the stability behaviour of local velocity profiles, temporal linear stability analysis has been performed. Assuming small velocity disturbances $\Phi(y)\exp(ia(x-ct))$ to a base profile $u(y)$, linearization leads to the Orr-Sommerfeld equation

$$(u-c)(\Phi''-\alpha^2\Phi)-u''\Phi = -\frac{i}{\alpha\,\mathrm{Re}}(\Phi''''-2\alpha^2\Phi''+\alpha^4\Phi). \qquad (5)$$

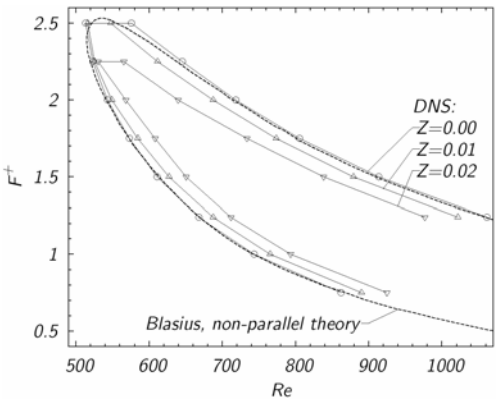

Figure 3: Curves of neutral stability for small values of Z obtained from DNS, and comparison with non-parallel theory (Herbert and Bertolotti, 1991).

Hereby, real values of α and the real part of c denote wave number and phase velocity of the disturbance, respectively. Negative imaginary parts of c then signal instability of the profile. The boundary conditions are that the disturbance and its first derivative have to vanish at y=0 and $y\rightarrow\infty$. We have implemented a Chebyshev tau method based on the modifications described by Gardner, Trogdon, and Douglas (1989) to avoid spurious eigenvalues. An exponential mapping x=2exp(-κy)-1 transforms between the semi-infinite wall-normal coordinate y and the Chebyshev interval [-1,1] of the new coordinate x, where κ denotes an additional mapping parameter. The discretization procedure results in a generalized eigenvalue problem of expansion order N-2 which is solved by a standard LAPACK procedure. Extensive resolution tests and validation runs for both the Blasius boundary layer profile and the exponential velocity profile have been performed ensuring the accuracy of the method. The critical Reynolds number of the exponential profile was found to $Re_{exp,c}$=47119.5 at a_c=0.16225 and c_r=0.15587 at N=102 and κ=0.1 which is in excellent agreement to other numerical results published in Lakin and Reid (1982).

RESULTS

2D Direct Numerical Simulation Results

In the absence of Lorentz forcing (Z=0), TS waves grow and decay corresponding to non-parallel linear stability theory reported by Herbert and Bertolotti (1991). Both branches of the neutral stability curve in Fig. 3 are well reproduced by our DNS. Already when applying weak Lorentz force amplitudes Z=0.01 and 0.02, the unstable region is reduced. At Z=0.05, TS waves of all investigated frequencies are damped within the computational domain. Figure 4 shows the behaviour of the growth rate vs. the downstream coordinate for three selected TS wave frequencies. For the uncontrolled case (lines marked with circles), the unstable region (σ>0) between branch I and II is clearly visible. In case of control at amplitude Z=1 (lines without markers), the corresponding growth rates are already reduced at x<0 because of a small upstream influence due to the elliptic nature of the Navier-Stokes equations. Beginning at the onset of control at x=0, σ sharply drops and reaches a minimum in a region 100<x<200. Further downstream, it again increases as the velocity profile approaches the exponential state. This

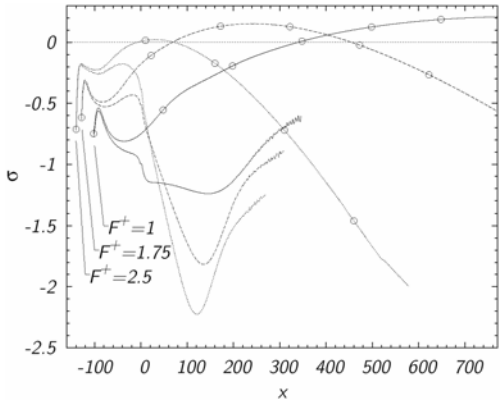

Figure 4: Evolution of TS wave growth rates for selected frequencies during transistion from Blasius to exponential profile. Lines with circles: Z=0, lines without markers: Z=1.

behaviour is observed for all investigated frequencies. Further downstream, below an $\hat{u}_{rms}$ level of 10^{-6}, the TS waves vanish in numerical noise.

Linear Stability Analysis Results

Linear stability analysis has been applied to velocity profiles extracted from the above DNS at several x in the absence of any disturbance input. As the Lorentz force is switched on at x=0, Fig. 5a) and b) show curves of neutral stability vs. Reynolds number at three different downstream locations. Upstream the Lorentz actuation at x=-100, the profile is close to the Blasius shape, resulting in a critical Reynolds number only slightly above $Re_{Blasius,c}$=519 (vertical dotted line). Far downstream, at x=700, the profile is almost exponential, resulting in a critical Reynolds number slightly above $Re_{exp,c}$ (vertical dotted line). However, downstream the onset of the force at x=100, the critical Reynolds number is clearly larger than $Re_{exp,c}$, that is Re_c increases non-monotonically. The corresponding velocity profiles and their deviations from the exponential profile are shown in Fig. 5c). As can be seen from Fig. 6a), the action of the Lorentz force leads to intermediate velocity profiles which are more stable than the asymptotic exponential profile. For a number of boundary layer flows, Fig. 6b) indicates a good correlation between the critical Reynolds number and the shape parameter H_{12}, the latter being defined as the ratio of displacement thickness to momentum thickness. However, the profiles near the onset of electromagnetic control differ remarkably.

3D Direct Numerical Simulation Results

For three-dimensional DNS, the domain extends over 26 units in spanwise direction where periodicity is assumed, allowing for a Fourier ansatz of up to 128 modes. The streamwise length is 320 units for Z=0, and 500 units for the remaining cases Z=0.1 and Z=0.2. Actuation starts 100 units downstream of the inflow, again at x=0. Inflow Reynolds number is Re_{in}=585. Transition to turbulence is initiated by introducing three-dimensional disturbances similar to Rist and Fasel (1995). Figure 7 shows vortex visualization by means of the λ_2-method (Jeong and Hussain, 1995) of the flow when applying different Lorentz force amplitudes. Due to the secondary instability mechanism, three-dimensional disturbances grow rapidly. While detailed effects of Lorentz forcing on secondary growth rates are currently under examination, the early

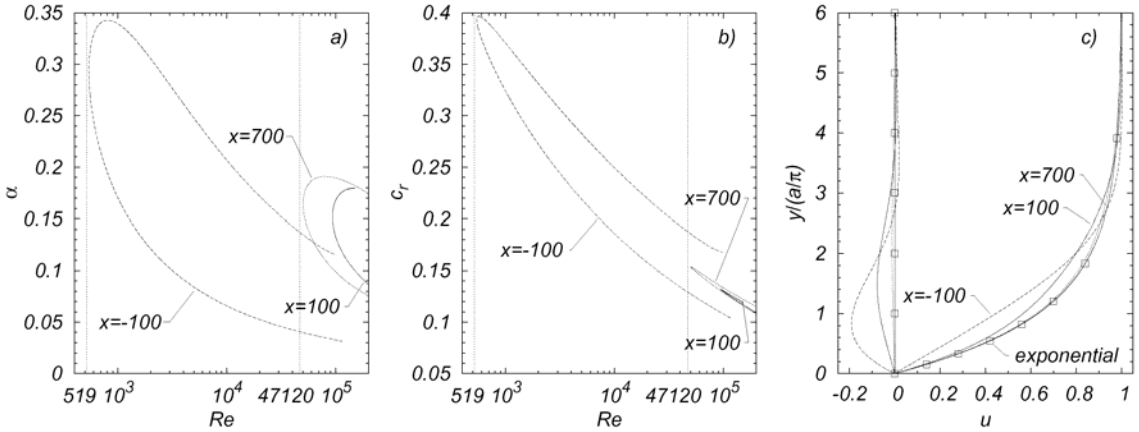

Figure 5: Curves of neutral stability vs. Reynolds number obtained from LSA for three velocity profiles: x=-100 (close to Blasius profile), x=100 (during transition) and x=700 (almost exponential). a) wave number α, b) phase velocity c_r. c) corresponding velocity profiles $u(y)$. At $u = 0$, additionally the deviation from the exponential profile is shown.

development of Λ-vortices appears almost unchanged in the present calculations. This is probably due to the late onset of forcing and rather dramatic secondary growth rates, however, the intensity (vorticity) of Λ-vortices lowers as Z is increased. In the uncontrolled case Ω-vortices emerge, followed by the usual breakdown to turbulence. Applying a moderate Lorentz force Z=0.1 delays this process, Λ-vortices are elongated and Ω-vortices appear further downstream. Finally, the flow becomes turbulent again. When further increasing the Lorentz force to Z≥0.2, Λ-vortices remain stable and dissipate downstream.

DISCUSSION

The numerical results presented confirm the expected increased stability since TS waves and late stage transitional structures are damped when Lorentz force is applied. Surprisingly, both DNS and LSA results suggest interesting stability characteristics of the investigated intermediate velocity profiles. In DNS, strongly decreasing growth rates are found near the onset of control. In this region, temporal LSA reports superior linear stability properties, which clearly differ from the monotonic behaviour of the critical Reynolds number versus shape parameter known so far. Although this method is limited in concluding on spatial stability of the boundary layer, it gives first ideas on the influence of the Lorentz force. Furthermore, the critical Reynolds number of 519 in temporal analysis is well reproduced by TS wave growth rates obtained from DNS, as shown in Fig. 1, which supports the relevance of the LSA results. We would also like to mention that critical Reynolds numbers larger than the one for the exponential profile have also been found in other problems (Zhilyaev et al., 1991).

CONCLUSION

Lorentz force actuation appears to be interesting for transition control. However, given the magnetic field strength available by today's permanent magnets, its practical application is currently limited due to significant power requirements for driving the electrodes. As the Lorentz force acts within the boundary layer, another appealing application of the actuator could be opposition control, where TS waves are damped by superposing antiphased waves, also as experimentally force amplitude and penetration depth may easily be adjusted. This typically requires power input being at least an order of magnitude lower.

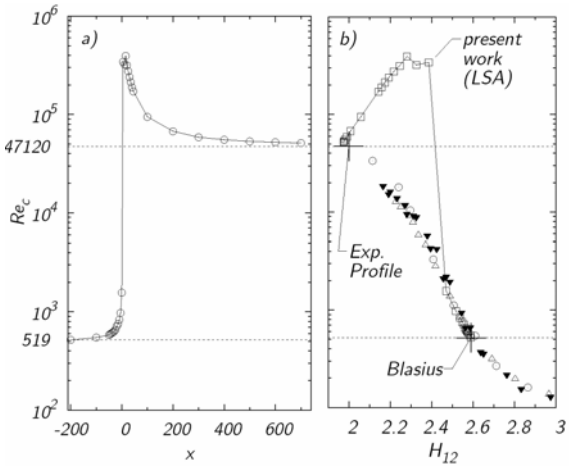

Figure 6: Critical Reynolds number a) vs. down-stream coordinate x, b) vs. shape parameter H_{12}. Experimental data (markers) taken from Wazzan et al. (1981).

REFERENCES

AVILOV, V. V. (1998), "Electric and magnetic fields for the Riga plate", Technical report, Internal report Rossendorf Research Center, Germany.

AVILOV, V. V., WEIER, T., MUTSCHKE, G. and GERBETH, G. (1999), "Optimal structure of EMHD boundary layer control plate", Technical report, Internal report Rossendorf Research Center, Germany.

DU, Y., SYMEONIDIS, V. and KARNIADAKIS, G. E. (2002), "Drag reduction in wall-bounded turbulence via a transverse traveling wave", *J. Fluid Mech.*, **457**, 1–34.

FASEL, H. F. (2002), "Numerical investigation of the interaction of the Klebanoff-mode with a Tollmien-Schlichting wave", *J. Fluid Mech.*, **450**, 1–33.

FRANSSON, J. and ALFREDSSON, P. (2003), "On the disturbance growth in an asymptotic suction boundary layer", *J. Fluid Mech.*, **482**, 51–90.

GAILITIS, A. and LIELAUSIS, O. (1961), "On a possibility to reduce the hydrodynamic resistance of a

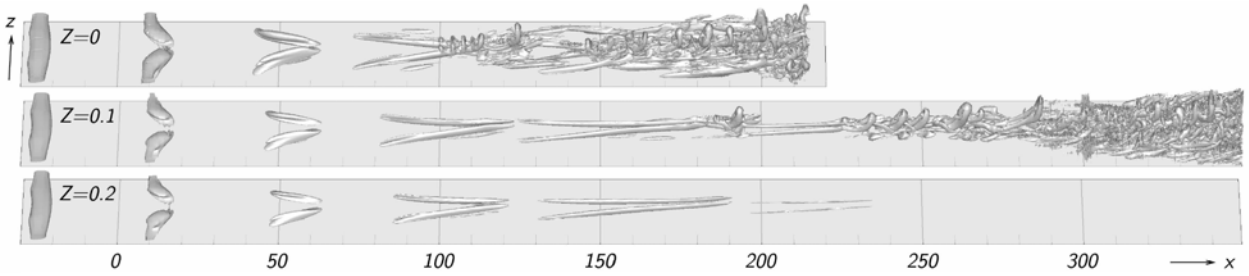

Figure 7: Coherent structures during transition to turbulence controlled by Lorentz force, for three different force amplitudes. Upper part: no control, middle: Z = 0.1, lower: Z = 0.2. Visualization by means of isosurfaces of the λ_2-criterion.

plate in an electrolyte", *Applied Magnetohydrodynamics, Reports of the Physics Institute Riga*, **12**, 143–146, in Russian.

GARDNER, D. R., TROGDON, S. A. and DOUGLAS, R. W. (1989), "A modified tau spectral method that eliminates spurious eigenvalues", *J. Comput. Phys.*, **80**, 137–167.

GUO, Y., ADAMS, N. A. and KLEISER, L. (1996), "A comparison study of an improved temporal DNS and spatial DNS of compressible boundary layer transition", *AIAA J.*, **34**, 683–690.

HENDERSON, R. and KARNIADAKIS, G. (1995), "Unstructured spectral element methods for simulation of turbulent flows", *J. Comput. Phys.*, **122**, 2, 191–217.

HERBERT, T. and BERTOLOTTI, F. P. (1991), "Stability analysis of nonparallel boundary layers", *Bull. Amer. Phys. Soc.*, **32**, 2079–XXXX.

JEONG, J. and HUSSAIN, F. (1995), "On the identification of a vortex", *J. Fluid Mech.*, **285**, 69–95.

JOSLIN, R. (1998), "Aircraft laminar flow control", *Ann. Rev. Fluid Mech.*, **30**, 1–29.

KNEISEL, E. (2004), "Boundary layer control by electromagnetic forces", Technical report, TU Dresden/FZ Rossendorf, in German, also available at www.tu-dresden.de/mwism/sm/projects/completed/1608-I.pdf.

LAKIN, W. and REID, W. (1982), "Asymptotic analysis of the Orr-Sommerfeld problem for boundary-layer flows", *Quart. J. Mech. appl. Math.*, **35**, 1, 69–89.

LEE, C. and KIM, J. (2002), "Control of the viscous sublayer for drag reduction", *Phys. Fluids*, **14**, 7, 2523–2529.

MOREAU, R. (1990), *Magnetohydrodynamics*, Kluwer Academic Publishers.

MUTSCHKE, G., GERBERT, G., ALBRECHT, T. and GRUNDMANN, R. (2006), "Separation control at hydrofoils using lorentz forces.", *Eur. J. Mech. B/Fluids*, **25**, 2, 137–152.

PANG, J. and CHOI, K.-S. (2004), "Turbulent drag reduction by Lorentz force oscillation", *Phys. Fluids*, **16**, 5, 35–38.

POSDZIECH, O. and GRUNDMANN, R. (2001), "Electromagnetic control of seawater flow around circular cylinders", *Eur. J. Mech. B/Fluids*, **20**, 255–274.

RIST, U. and FASEL, H. (1995), "Direct numerical simulation of controlled transition in a flat-plate boundary layer", *J. Fluid Mech.*, **298**, 211–248.

TSINOBER, A. B. and SHTERN, A. G. (1967), "Possibility of increasing the flow stability in a boundary layer by means of crossed electric and magnetic fields", *Magnitnaya Gidrodinamika*, **3**, 2, 152–154.

ULRICH, A. (1944), "Theoretische untersuchungen über die widerstandsersparnis durch laminarhaltung mit absaugung.", *Schriften d. dt. Akad. d. Luftfahrtforschung*, **2**, 8B, 53–91.

WAZZAN, A. R., GAZLEY, C. and SMITH, A. M. O. (1981), "H-r_x method for predicting transition", *AIAA J.*, **19**, 6, 810–812.

ZHILYAEV, M. I., KHMEL, T. A. and YAKOVLEV, V. I. (1991), "Boundary-layer stability in magnetohydrodynamic streamlining of a plate with an internal source of electromagnetic fields", *Magnitnaya Gidrodinamika*, **27**, 2, 76–83, in Russian.